Effect of Particle Loading on Microealstic Behavior and interfacial Tractions of Boron Carbide/AA4015 Alloy Metal Matrix Composites

A. Chennakesava Reddy

Assistant Professor, Department of Mechanical Engineering, MJ College of Engineering and Technology, Hyderabad, India
dr_acreddy@yahoo.com

Abstract: A micromechanical approach is developed to determine the micro stress within a metal matrix composite under various particle loading conditions. Square diamond unit cell/ round particle RVE models are analyzed and compared using two-dimensional finite element methods for Boron carbide/AA4015 alloy metal matrix composites. Subsequently, effective material properties, the distribution of micro stress in the particle/matrix, as well as traction distribution at the particle–matrix interface, and the effect of different interfacial stiffness, are obtained.

Keywords: AA4015 alloy, boron carbide, RVE model, finite element analysis, interfacial tractions.

1. INTRODUCTION

Micromechanical methods have been widely used for decades to study stress/strain distributions within composites, as well as the correlation between constituent properties and macro (effective) properties of composite materials. The homogeneous boundary conditions, i.e., 'plane remains plane' during the deformation of a unit cell, are over-constrained for shear loading [1-2]. Several publications concerning the FEA of composites can be found in the literature. Presently, the use of a representative volume element (RVE) or a unit cell [3] of the composite microstructure, in conjunction with a finite element (FE) analysis tool is well recognized for determining the effective material properties and understanding the micromechanics of the composite materials.

The aim of the present paper is to establish the influence of particle loading of boron carbide as reinforcement material and interfacial tractions in boron carbide.AA4015 alloy metal matrix composites. Finite element analysis (FEA) of B_4C/AA4015 alloy metal matrix composites was executed RVE models comprising of square diamond cell/round particle.

2. MATERIALS AND METHODS

The matrix material was AA4015 alloy. The loading of boron carbide particulate reinforcement were 10%, 20%, and 30%. The RVE scheme with perfect adhesion of boron carbide particles with AA4015 alloy matrix was applied as shown in figure 1. The PLANE183 element was used for the matrix and the nanoparticle. The interface between particle and matrix was discretized using a COMBIN14 spring-damper element.

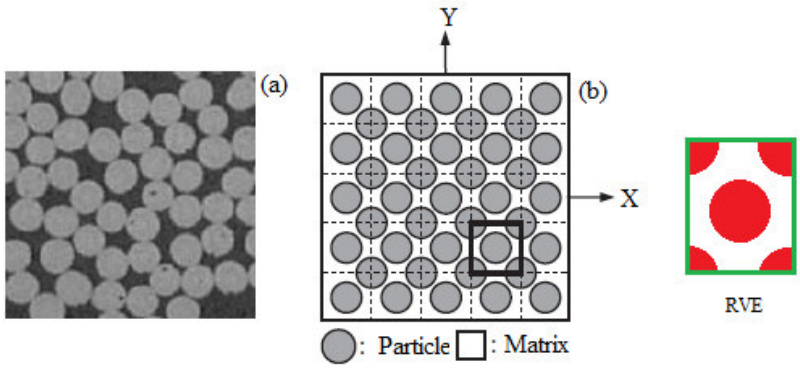

Figure 1: The RVE model: (a) particle distribution, (b) consideration for diamond cell/round particle and (d) RRVE scheme.

A linear stress–strain relation at the macro level can be formulated as follows:

$$\bar{\sigma} = \bar{C}\bar{\varepsilon} \quad (1)$$

where $\bar{\sigma}$ is macro stress, and $\bar{\varepsilon}$ represents macro total strain and $\bar{C}$ and is macro stiffness matrix.

For plane strain conditions, the macro stress- macro strain relation is as follows:

$$\begin{Bmatrix} \overline{\sigma_x} \\ \overline{\sigma_y} \\ \overline{\tau_{xy}} \end{Bmatrix} = \begin{bmatrix} \overline{C_{11}} & \overline{C_{12}} & 0 \\ \overline{C_{21}} & \overline{C_{22}} & 0 \\ 0 & 0 & \overline{C_{33}} \end{bmatrix} \times \begin{Bmatrix} \overline{\varepsilon_x} \\ \overline{\varepsilon_y} \\ \overline{\gamma_{xy}} \end{Bmatrix} \quad (2)$$

The tractions at the particle–matrix interface can be expressed in terms of the macro stresses. As in figure 4, traction t at any point on the interface can always be decomposed into three components: normal traction t_n, which is perpendicular to the interface at the current point, tangential traction t_t which is tangent to the circumference of the particle at the current point, and longitudinal traction t_z which is parallel to the longitudinal direction of the particle. By simple transformation of coordinates, interfacial tractions at one point located at the particle–matrix interface can be computed from micro stresses at an adjacent point belonging to the matrix. The interfacial tractions can be obtained by transforming the micro stresses at the interface as given in Eq. (3):

$$t = \begin{Bmatrix} t_z \\ t_n \\ t_t \end{Bmatrix} = T\sigma \quad (3)$$

where, $T = \begin{bmatrix} 0 & 0 & 0 \\ cos^2\theta & sin^2\theta & 2sin\theta cos\theta \\ -sin\theta cos\theta & sin\theta cos\theta & cos^2\theta - sin^2\theta \end{bmatrix}$

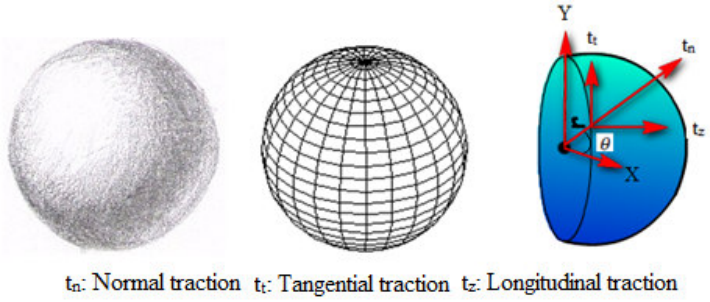

Figure 2: Schematic representation of interfacial traction vector.

3. RESULTS AND DISCUSSION

Figure 3 represents the effective material properties of B_4C/AA4015 alloy metal matrix composites attained by FEA. As volume fraction increases, Ex also increases. However, the transverse elastic modulus Ey decreases slightly as volume fraction increases (figure 3a). The major Poisson's ratio, v_{12} increases with increase of volume fraction (figure 3b). Since elastic modulus of boron carbide particle in the longitudinal direction is much greater than that of the matrix, particle dominates the longitudinal stiffness (Ex) of the composite. The shear modulus decreases with increase of volume fraction boron carbide in the composite (figure 3c).

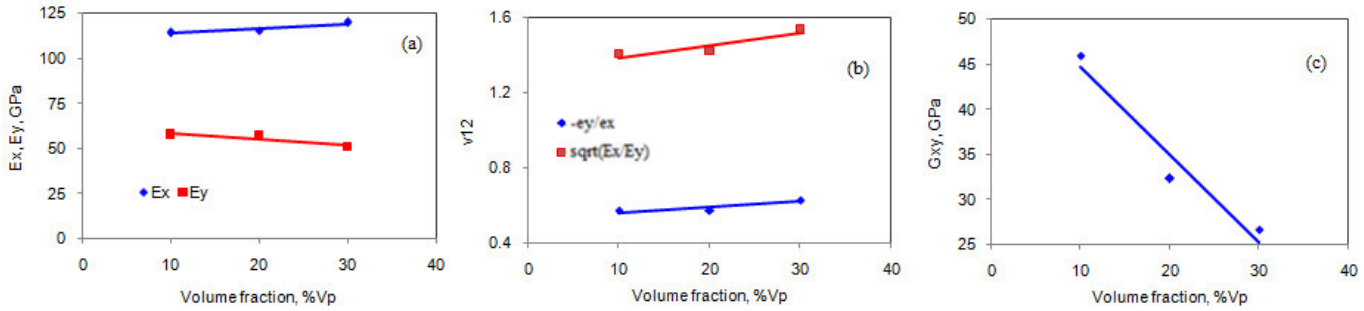

Figure 3: Effect of volume fraction on effective material properties.

Figure 4 shows tensile strains developed in a unit cell of square diamond array under tensile stress. In a unit cell of square diamond array under tensile stress, maximum stress concentration can be observed in the neighboring region of the particle–matrix interface, along the loading direction. The strains are high in the particles along transverse direction of loading due to compression of particles. Two regions of maximum stress concentration are located near the interface on either side of the

particle along the load direction (figure 5). The maximum shear strains and stresses are occurred at 45°, 135°, 225° and 315° at the interface (figure 6). As shown in the von Mises stress plots, the regions of minimum stress concentration align with transverse direction of tensile loading (figure 7).

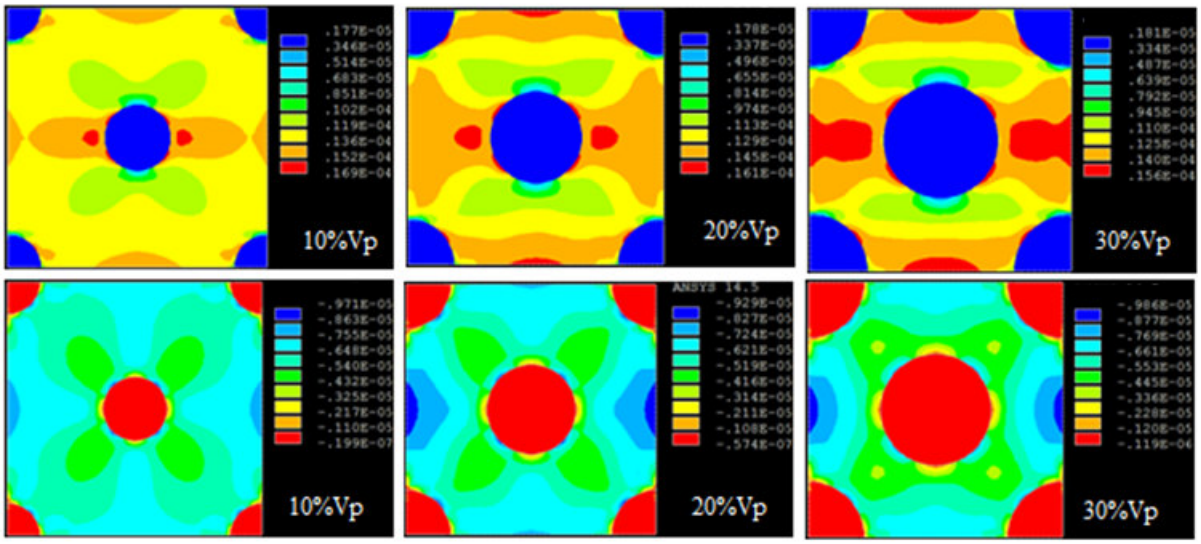

Figure 4: Elastic strain developed in B_4C/AA4015 alloy metal matrix composites: ε_x and (b) ε_y.

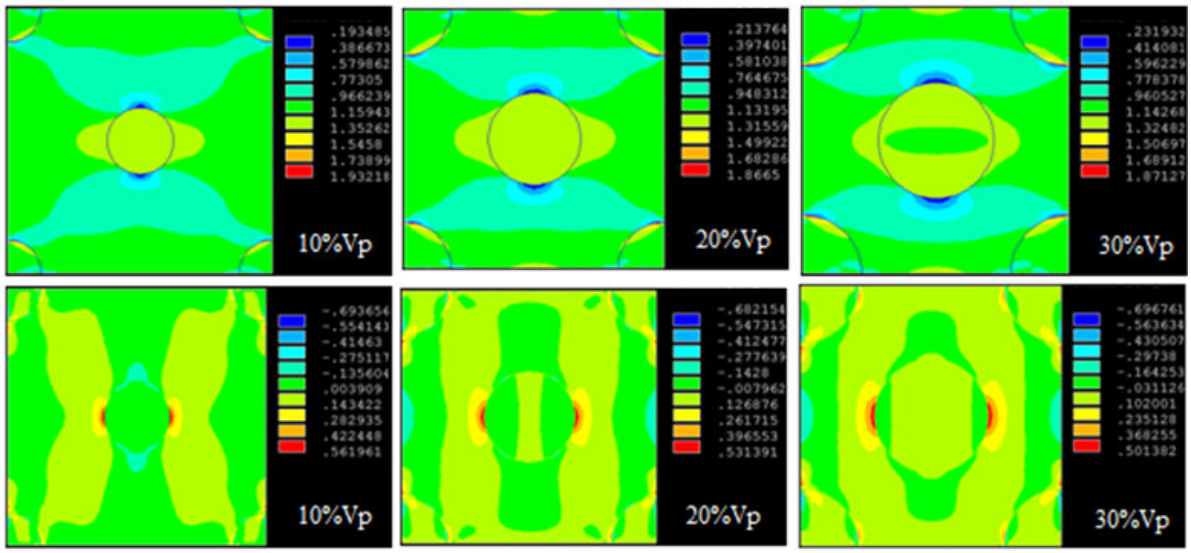

Figure 5: Tensile stress induced in B_4C/AA4015 alloy metal matrix composites: σ_x and (b) σ_y.

The normal and tangential tractions at the particle–matrix interface of unit cells subject to tensile stress are calculated for volume fractions ranging from 0.1 to 0.3. The longitudinal traction is zero for the particle reinforcement with the plane strain conditions. In figure 8(a), it can be observed that the value of normal traction, t_n decreases as θ increases from 0° to 150° in the unit cells. The direction of macro load coincides with the direction of t_n at θ =0°, so t_n attains its maximum; as θ increases, the component of the macro load in the normal direction of the interface decreases, so t_n also decreases. As for tangential traction t_t, whose variation with θ is shown in figure 8(b), its value decreases as θ increases from 0°, and reaches the minimum at 30° and then increases until θ =120°.

4. CONCLUSION

A micromechanics approach is developed to explicitly express the relationship between macro stress and micro stress for B_4C/AA4015 alloy metal matrix composites. For effective material properties, variations of Ex, E_y, G_{xy} and v_{12} with respect to V_p, are predicted. Additionally, in unit cells with different particle volume fractions, variations of interfacial tractions along

particle perimeter under tension loading. In a unit cell of square array under tensile stress, maximum stress concentration can be observed in the neighboring region of the particle–matrix interface, along the loading direction.

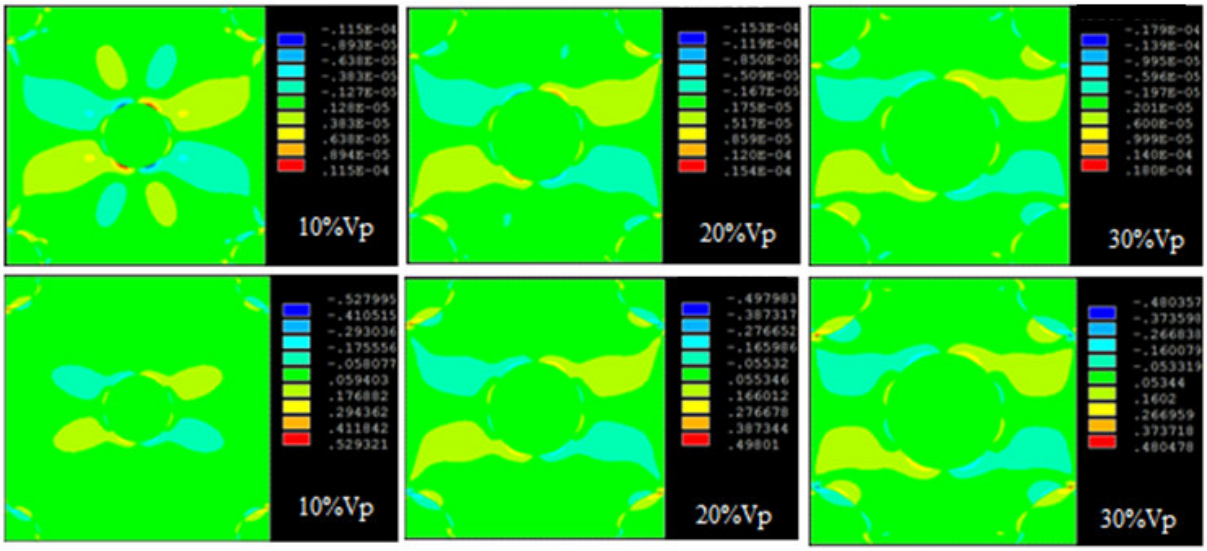

Figure 6: Shear strains (a) and shear stress in B_4C/AA4015 alloy metal matrix composites.

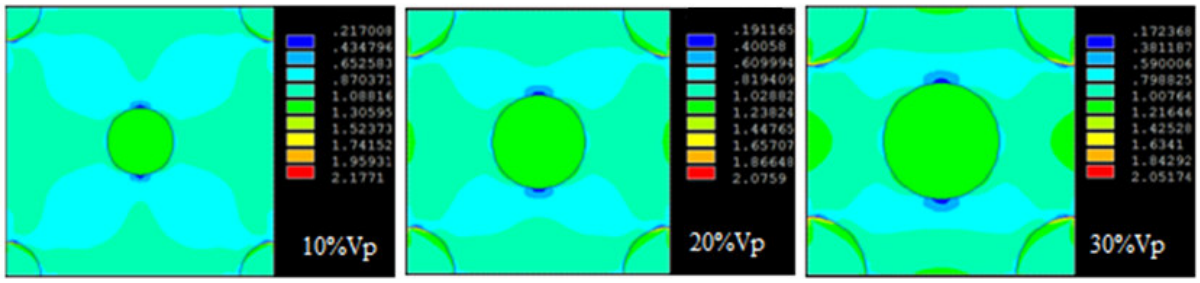

Figure 7: von Mises stress induced in B_4C/AA4015 alloy metal matrix composites.

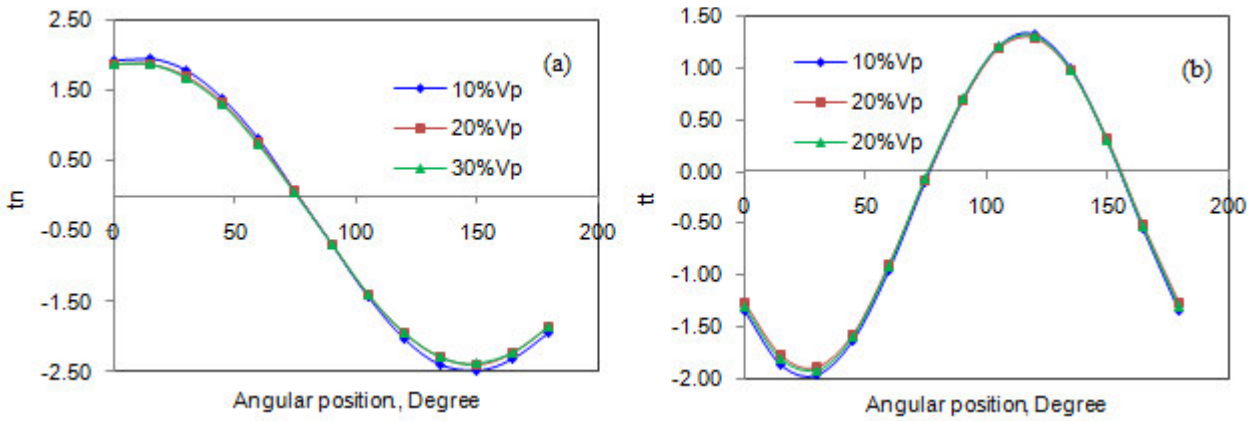

Figure 8: Interfacial tractions along the angle due to tensile loading: (a) longitudinal and (b) tangential.

REFERENCES

1. R Hill. Elastic properties of reinforced solids: some theoretical principles. J. Mech. Phys. Solids, vol. 11, pp. 357-372, 1963.
2. P. Suquet, Elements of Homogenization Theory for Inelastic Solid Mechanics, In: Homogenization Techniques for Composite Media, Springer-Verlag, Berlin, pp. 194–275, 1987.
3. J. Aboudi, Mechanics of Composite Materials, A Unified Micromechanical Approach, Elsevier, Amsterdam, 1991.